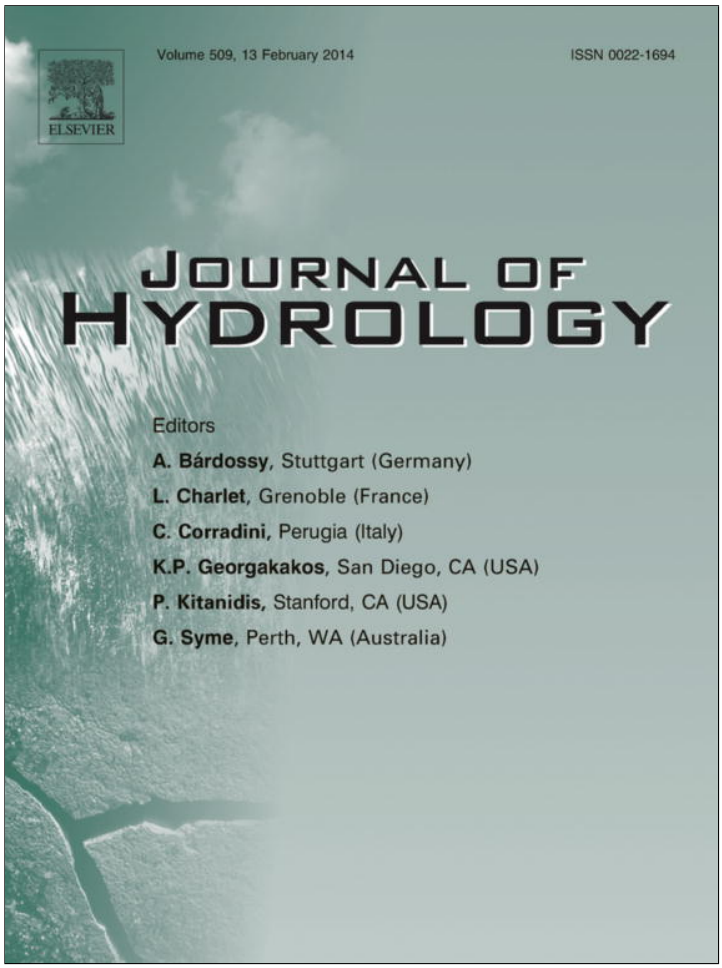

Journal of Hydrology 509 (2014) 416–429

Contents lists available at ScienceDirect

Journal of Hydrology

journal homepage: www.elsevier.com/locate/jhydrol

Three-dimensional aquifer inversion under unknown boundary conditions

Ye Zhang [a,*], Juraj Irsa [b], Jianying Jiao [a]

[a] Department of Geology and Geophysics, University of Wyoming, Laramie, WY, USA
[b] Schlumberger, Inc., Houston, TX, USA

ARTICLE INFO

Article history:
Received 16 August 2013
Received in revised form 6 November 2013
Accepted 15 November 2013
Available online 26 November 2013
This manuscript was handled by Corrado Corradini, Editor-in-Chief, with the assistance of Aldo Fiori, Associate Editor

Keywords:
Aquifer
Inverse method
Hydraulic conductivity
Non-uniqueness
Boundary conditions

SUMMARY

A new method for three-dimensional steady-state aquifer inversion is developed to simultaneously estimate aquifer hydraulic conductivities and the unknown aquifer boundary conditions (BC). The method has its key strength in computational efficiency, as there is no need to fit an objective function, nor repeated simulations of a forward flow model. It employs a discretization scheme based on functional approximations and a collocation technique to enforce the global flow solution. The noisy observed data are directly incorporated into the inversion matrix, which is solved in a one-step procedure. The inverse solution includes hydraulic conductivities and head and flux approximating functions from which the model BC can be inferred. Thus a key advantage of the method is that it eliminates the non-uniqueness associated with parameter estimation under unknown BC which can cause the result of inversion sensitive to the assumption of aquifer BC. Two approximating functions are tested here, one employing quadratic approximation of the hydraulic head (flux is linear), the other cubic approximation. Two different BC are also tested, one leading to linear flow, the other strongly nonlinear flow. For both BC, the estimated conductivities converge to the true values with grid refinement, and the solution is accurate and stable when a sufficient number of the observation data is used. Compared to the quadratic function, the cubic function leads to a faster convergence of the estimated conductivity at a lower level of grid discretization, while it is also more robust for the different flow conditions tested. A sensitivity analysis is conducted whereby the inversion accuracy is evaluated against data density. Composite scale sensitivity (CSS) can reveal the overall information content of the data. However, when the number of measurements is fixed, CSS cannot reveal whether the observed data can lead to reliable conductivity estimates. A one-observation-at-a-time (OAT) approach is proposed, which can indicate the reliability of the estimated conductivity for a given set of the observation data. To evaluate the stability of the method when the observation data contain errors, a problem with 4 hydrofacies conductivities is inverted using hydraulic heads and a single Darcy flux component. The results are accurate when the measurement error is small but become slightly less accurate when the error is larger. In summary, flow condition, inverse formulation, grid discretization, observation data density and location, and measurement errors all influence the accuracy of inversion.

1. Introduction

Hydraulic conductivity (K) is a critical parameter influencing fluid flow and solute transport in aquifers. However, estimation of aquifer hydraulic conductivity is a challenging task, due to issues related to aquifer heterogeneity, parameter and measurement scale effect, uncertainty in aquifer boundary conditions, and the lack of efficient estimation techniques. This study presents a three-dimensional (3D) steady-state inverse method which efficiently and simultaneously estimates aquifer hydraulic conductivities, flow field, and the unknown aquifer boundary conditions (BC). In the following paragraphs, different approaches of estimating aquifer hydraulic conductivity are briefly reviewed, before key features of the new method are presented and contrasted with the existing inverse methodology.

Aquifer K can be measured directly with Darcy tests on oriented cores or estimated using aquifer tests, indirect means, or via the calibration of an aquifer simulation model. Typically, core conductivity measurements sample a small aquifer volume, leading to values that are not representative of the aquifer at larger scales. With slug tests, K can be estimated for a greater volume using analytical flow solutions developed assuming radial flow from the test well in a homogeneous formation with an infinite lateral extent. Similarly, with pumping tests, analytical flow solutions have been developed

* Corresponding author. Tel.: +1 307 766 2981; fax: +1 307 766 6679.
E-mail address: yzhang9@uwyo.edu (Y. Zhang).

0022-1694/$ - see front matter © 2013 Elsevier B.V. All rights reserved.
http://dx.doi.org/10.1016/j.jhydrol.2013.11.024

to estimate large-scale horizontal hydraulic properties, e.g., the well-known Thiem solution for analyzing steady-state flow and the Theis solution for analyzing transient flow (Fitts, 2013). To obtain K at higher resolutions, the analytical functions can be applied to specific aquifer intervals that are isolated from the other intervals, e.g., borehole flowmeter test, multilevel slug test, direct-push permeameter test (Molz et al., 1994; Butler, 2005; Bohling et al., 2012). Compared to the K derived from core measurement and pumping test, these measurements can sample an intermediate range of the formation volume. Moreover, at the same core scale or well-test intervals, indirect K measurements can be made based on correlations between rock petrophysical properties and fluid flow properties, e.g., magnetic resonance logs, acoustic, density, or neutron logs, and electrical-conductivity profiling (Williams et al., 1984; Tang and Cheng, 1996; Shapiro et al., 1999; Hyndman et al., 1994, 2000; Schulmeister et al., 2003; Kobr et al., 2005; Camporese et al., 2011). For quality control, these indirect measurements are compared and combined with one or more direct K measurements. However, correlation between fluid flow and petrophysical properties is often site-specific and empirical in nature. To address this issue, joint inversion techniques have been developed whereas aquifer hydrodynamic data are analyzed jointly with geophysical measurements (Kowalsky et al., 2006; Brauchler et al., 2012). In these analyses, explicit correlation functions are not needed, although certain "structure similarity" between fluid flow and petrophysical properties is enforced to help constrain the joint inversion.

Another type of indirect K measurement can be made by building and calibrating an aquifer simulation model with an inverse method (Hill and Tiedeman, 2007). For an overview of the inverse methodologies used in groundwater model calibration, including both direct and indirect methods and their pros and cons, please see Neuman and Yakowitz (1979), Weir (1989), and Irsa and Zhang (2012). Within the inversion framework, K becomes a model calibration parameter and can be estimated (or inverted) at different scales of interest. For example, aquifer flow models with distinct hydrofacies zones can be built for which K can be estimated for each hydrofacies. In highly parameterized inversion, K can be estimated for each grid cell by imposing additional constraint equations on the inverse formulations (Zimmerman et al., 1998; Doherty, 2005; Liu and Kitanidis, 2011). However, most of the existing inverse techniques are based on minimizing an objective function, which is typically defined as a form of mismatch between the measurement data and the corresponding model simulated values. During inversion, to minimize the objective function, parameters including conductivities are updated iteratively using a forward model which provides the linkage between the parameters and the data. Because a forward model is needed, boundary conditions (BC) of the model are commonly assumed known, or less frequently, calibrated during the inversion. However, BC of natural aquifers are often unknown or uncertain. (In transient problems, both aquifer initial and boundary conditions are unknown.) As demonstrated by Irsa and Zhang (2012), different combinations of parameters and BC can lead to the same objective function values, thus results of many existing techniques may become non-unique.

To address non-uniqueness in K estimation, Irsa and Zhang (2012) developed a novel steady-state direct method for inverting two-dimensional (2D) confined aquifer flow. The method adopts a set of approximating functions of hydraulic heads and groundwater fluxes as the fundamental solutions of inversion. It does not rely on minimizing objective functions (i.e., forward model-data mismatch), while hydraulic conductivity, flow field, and the unknown aquifer BC can be simultaneously estimated. Synthetic aquifer problems with regular and irregular geometries, different (deterministic) hydrofacies patterns, variances of heterogeneity, and error magnitudes were tested. In all cases, K converged to the true or expected values and was therefore unique, based on which heads and flow fields were reconstructed directly via the approximating functions. Boundary conditions were then inferred from these fields. In the 2D analysis, the inversion accuracy was demonstrated to improve with increasing observed data, low measurement errors, and grid refinement, although source/sink effects cannot be accommodated. To address the source/sink effects (e.g., pumping and recharge), Zhang (submitted for publication) extended the technique to inverting unconfined aquifers by superposing analytical flow solutions to generate the approximating functions. In these cases, the inverse solution was obtained via nonlinear optimization while the same high computation efficiency was maintained. Furthermore, to account for uncertainty in inversion due to the uncertain hydrofacies patterns, the method was combined with geostatistical simulation, whereas both K uncertainty and uncertainty in the unknown aquifer BC can be quantified (Wang et al., 2013).

This study extends our earlier works by demonstrating the applicability of the new direct method to inverting three-dimensional (3D) steady-state flow in confined aquifers. Similar to our earlier works, the 3D algorithm is tested using a set of synthetic forward (true) models which provide the measurement data, with or without measurement errors, for inversion. However, unlike the earlier works, the inversion accuracy is tested using two different sets of (increasingly complex) approximating functions under two different global flow BC which induce either linear or strongly nonlinear flow. Again, BC of the forward models are assumed unknown and are estimated by inversion along with the hydraulic conductivities and the flow field. To assess the accuracy of inversion, the estimated conductivities and the BC are compared to those of the forward models. A sensitivity analysis is conducted to evaluate how the inversion outcomes converge to the true model with grid refinement or with increasing observation data. The issue of data worth is examined using different statistical measures. The stability of the method is also examined when measurement errors are increased from error-free to a set of realistic values. The inverse solution is considered stable if the estimated hydraulic conductivities do not vary from the true values by more than one orders of magnitude.

In the reminder of this article, non-uniqueness in parameter estimation under unknown aquifer BC is first illustrated, before the 3D inverse formulation of this study is introduced. Results are presented in four sections relating to: (1) convergence of the inverse algorithm with grid refinement; (2) data needs; (3) information content of the observations; and (4) stability of inversion under increasing measurement errors. In addressing topics (1)–(3), a homogeneous aquifer problem is inverted and the observation data include hydraulic heads and a single groundwater flow rate. In addressing topic (4), inversion is carried out for a heterogeneous problem with 4 hydrofacies. In this case, observation data include hydraulic heads and a single Darcy flux component. The relevant results are discussed before conclusion and future research are summarized at the end.

2. Non-uniqueness in parameter estimation

The determination of hydraulic conductivity for steady-state groundwater flow is mainly driven by the indirect inverse methods solving a set of boundary value problems to minimize an objective function. These methods assume either known BC for a given problem, or by appropriate parameterizations, obtain optimized BC during inversion which is typically an iterative procedure. The earlier generation of direct inversion methods (e.g., see a review in Sun (1994)) make similar assumptions about the BC, although

boundary conditions of real aquifers are rarely known in advance. In this section, we demonstrate that unknown aquifer BC can lead to non-uniqueness in the estimated hydraulic conductivities (*Ks*). For simplicity, a 2D example is presented here by calibrating a subdomain problem (see the box labeled 'a–b–c–d' in Fig. 1a) of a larger forward model. A set of true *Ks* and BC are specified to this larger model (Fig. 1a), which is simulated with MODFLOW2000 (Harbaugh et al., 2000). The finite difference forward model (FDM) and its discretization is shown in Fig. 1a. From the subdomain of this model, a set of regularly spaced observation data (18 heads and 4 Darcy fluxes) is sampled without any measurement errors. Based on these data, two hydrofacies conductivities (*K*2, *K*3) that lie within the subdomain is calibrated with PEST (Doherty, 2005) and with the direct method (Irsa and Zhang, 2012). For both methods, the inversion domain is defined by the box-shaped subdomain within which all the observation data lie. The subdomain BC are unknown to the new method, but are assumed known to PEST with increasing degrees of uncertainty. To both methods, the *location* of the larger FDM boundaries as well as their BC are unknown, which is typical of real-world problems where the measurement site may lie far from the aquifer boundaries. Because only deterministic (zoned) inversion is tested and compared here, the pattern of conductivities within the subdomain is assumed known to both methods.

For inversion with the direct method, a 3×2 inverse grid is used to represent the subdomain (not shown). This small grid size gives rise to a very small inversion system of equations, which can be solved efficiently, i.e., the inverse code is written with MATLAB 2012a for which the computation time to solve this problem is less than one second on a PC workstation. Given the set of error-free observed data, the estimated *Ks* are extremely close to the true values with the estimation errors that are less than 1% (Table 1). The inversion also recovers the hydraulic heads along the subdomain boundaries (as well as heads internal to these boundaries), which are compared to the true "BC", i.e., heads sampled from the larger FDM along the subdomain boundaries (Fig. 1b). With the direct method, *K*2, *K*3 and the BC can be accurately and simultaneously estimated.

For inversion with PEST, forward simulations of steady-state flow within the subdomain are needed. This forward model, also

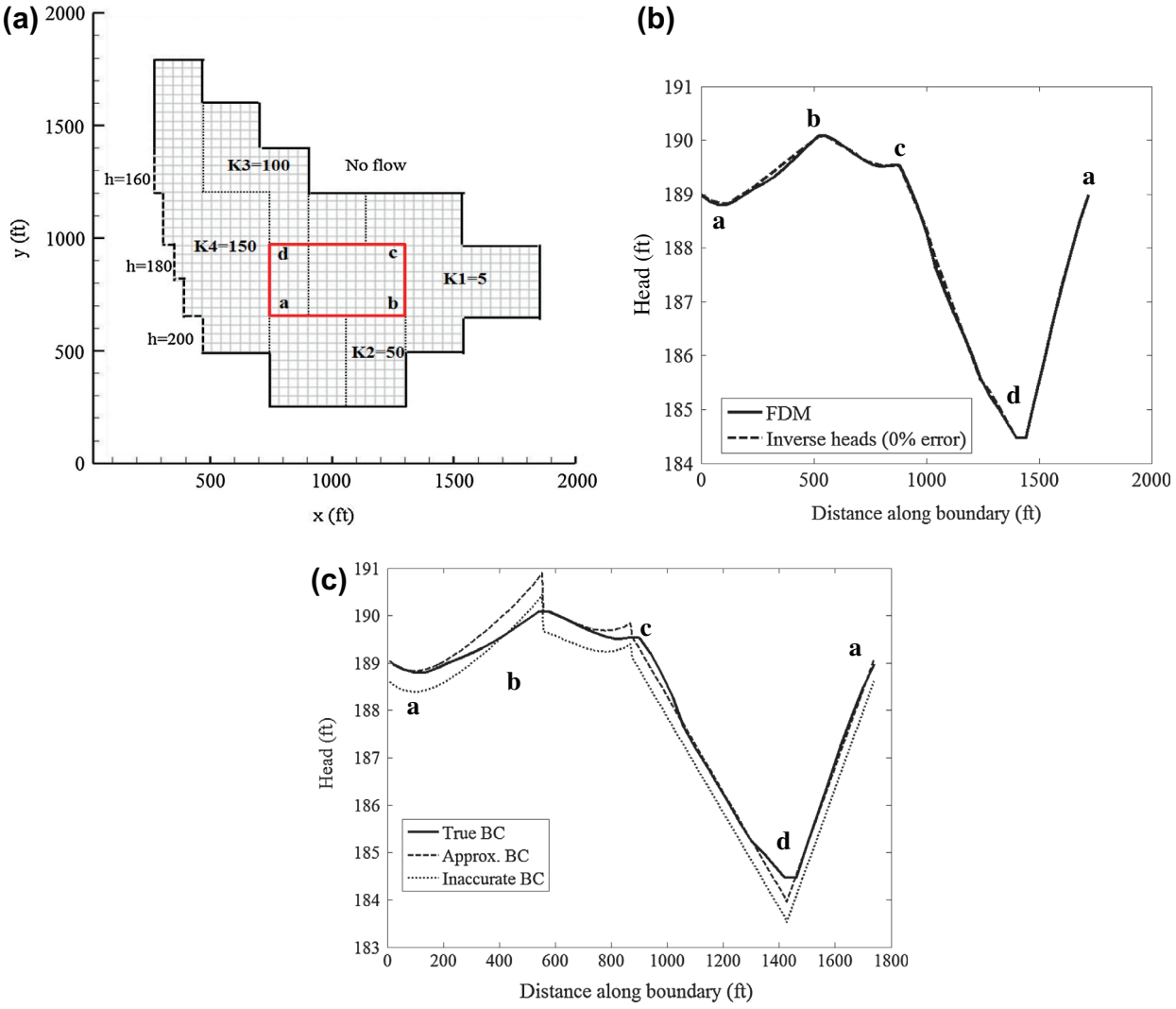

Fig. 1. (a) The larger finite difference model (FDM) and the subdomain ('a–b–c–d') where the aquifer dynamic data are sampled for inversion. The BC of the FDM are shown: besides the inflow and outflow boundaries, the remaining boundaries are no-flow. (b) Hydraulic heads along the subdomain boundaries are computed by the FDM and are referred to as the "True BC" (thick solid line). Heads along the same boundaries inverted by the direct method with error-free measurements are referred to as "Inverse heads" (thick dash line). (c) Based on the True BC, two increasingly perturbed sets of BC ("Approx. BC" and "Inaccurate BC"; thin dash and dotted lines) are given to PEST for the estimation of *K*2 and *K*3 of the subdomain.

Table 1
Estimated hydraulic conductivities (ft/d) for the subdomain using the direct method and using PEST under 3 different sets of assumed subdomain BC.

	Grid	Conductivity		BC
		*K*2	*K*3	
True model (subdomain)	14 × 8	50	100	True BC sampled from the larger FDM
PEST	40 × 40	46.6	105.9	True BC given to PEST (i.e., to create a forward model)
PEST	40 × 40	90.4	54.8	Approx. BC given to PEST
PEST	40 × 40	10,000	0.1	Inaccurate BC given to PEST
Direct method	3 × 2	49.8	100.7	Estimated by inversion

computed with MODFLOW2000, is extracted from the larger FDM and is discretized with a finer 40 × 40 grid (the original discretization in the FDM is 14 × 8). To generate the initial guess for PEST's iterations, true *K*2 and *K*3 values are given as the starting parameter values. To run the forward model, different BC are *postulated* along the subdomain boundaries (Fig. 1c), which lead to very different calibration results (Table 1). When the postulated BC are identical or close to the true BC ("True BC" and "Approx. BC" in Fig. 1c, respectively), the estimated *Ks* are either the true values or not far from the true values (Table 1). However, when a more perturbed set of BC is given to PEST ("Inaccurate BC"), the estimated *Ks* become quite inaccurate and fall at the parameter bounds provided to inversion even though their true values are used as the starting parameters. The case presented here reflects an extreme situation where wells are drilled and sampled for hydraulic heads along the entire model boundaries. Even if such a sampling scheme can be practically accommodated, the BC provided to inversion likely will contain measurement errors. Clearly, whether PEST can accurately recover the parameters will depend on how high these BC errors are.

For the problem examined here, the new inverse method yields "unique" outcomes while PEST results are sensitive to the assumed BC. This comparison illustrates the promise of the new method for uniquely estimating hydraulic conductivities when aquifer BC are unknown or uncertain. For the given (assumed known) parameterization, inversion with the new method can also obtain the correct BC, which suggests that it has a potential to be combined with the objective-function-based techniques to help reduce the non-uniqueness in parameter estimation. Further development and verification of the method for three-dimensional aquifer inversion is clearly desired and is the focus of the current study.

3. Direct method

The direct method of this study discretizes the model domain into block elements where a state variable is approximated with functions satisfying the local governing flow equation a priori, i.e., the fundamental solutions. Specifically, hydraulic head of each element is approximated by a function satisfying the Laplace's equation, and Darcy flux components are obtained from differentiating the head function via Darcy's Law. The inverse solution is obtained via minimizing a set of residual equations that are written at a set of collocation points placed at the element interfaces. Residual equations are also written at the observation locations, whether they are observed (point-scale) heads, observed (point-scale) fluxes, or observed flow rates. The unknown hydraulic conductivity is estimated together with the parameters of the head and flux approximating functions. The direct method does not require a prior knowledge of the aquifer BC, nor does it attempt to fit the BC during inversion. For a given problem, the aquifer BC are always assumed unknown. Together with the aquifer hydraulic heads and conductivities, the BC are part of the inverse solution. Furthermore, should the BC be known along a part of or along the entire model boundaries, the BC data (be they heads, fluxes, or flow rates) can be directly incorporated into the inversion as a set of observation data.

3.1. Approximating functions

The equation describing 3D steady-state groundwater flow in a heterogeneous confined aquifer without source/sink effect is:

$$\begin{aligned} &\nabla \cdot (\boldsymbol{q}) = 0 \\ &\boldsymbol{q} = -K(x,y,z)\nabla h \end{aligned} \tag{1}$$

where ∇ is the gradient operator, h is hydraulic head, $K(x,y,z)$ is locally isotropic, and $\boldsymbol{q}$ is Darcy flux. Given Eq. (1), the hydraulic head solution is a harmonic function within a homogeneous sub-region of the model domain, e.g., a single inverse grid element or a hydrofacies zone comprising of a number of elements. In this study, $K(x,y,z)$ is parameterized as discrete hydrofacies zones. For a given sub-region, the solution to the flow equation can be formulated by adopting a set of approximating functions of hydraulic head and Darcy fluxes. While the 2D studies of Irsa and Zhang (2012) tested a quadratic head approximating function in which case the flux approximation is linear, here we test two sets of functions with increasing orders of approximation, i.e., quadratic head $\tilde{h}_q$:

$$\begin{aligned} \tilde{h}_q(x,y,z) = {} & a_0 + a_1x + a_2y + a_3z + a_4xy + a_5xz + a_6yz + a_7(x^2 \\ & - z^2) + a_8(y^2 - z^2) \end{aligned} \tag{2}$$

and cubic head $\tilde{h}_c$:

$$\begin{aligned} \tilde{h}_c(x,y,z) = {} & a_0 + a_1x + a_2y + a_3z + 3a_4(x^2 - z^2) + 3a_5(y^2 - z^2) \\ & + 6a_6xy + 6a_7xz + 6a_8yz + 6a_9xyz + a_{10}x(3y^2 \\ & - x^2) + a_{11}x(3z^2 - x^2) + a_{12}y(3x^2 - y^2) + a_{13}y(3z^2 \\ & - y^2) + a_{14}z(3x^2 - z^2) + a_{15}z(3y^2 - z^2) \end{aligned} \tag{3}$$

For both cases, Darcy flux components are approximated as: $\tilde{q}_x = -K\frac{\partial \tilde{h}_c}{\partial x}, \tilde{q}_y = -K\frac{\partial \tilde{h}_c}{\partial y}, \tilde{q}_z = -K\frac{\partial \tilde{h}_c}{\partial z}$.

In the above equations, sub-indexes q and c indicate the order of approximation in the hydraulic head, while $a_0, a_1, \ldots, a_{15}$ are the unknown coefficients that will be determined from the inverse solution. In the model domain, each block element has 4 approximating functions $(\tilde{h}^{(k)}, \tilde{q}_x^{(k)}, \tilde{q}_y^{(k)}, \tilde{q}_z^{(k)})$, with 9 unknown coefficients for the quadratic head approximation and 16 unknown coefficients for the cubic head approximation. The corresponding level of approximation for the Darcy flux is linear if $\tilde{h}_q$ is adopted and quadratic if $\tilde{h}_c$ is adopted.

3.2. Continuity at the Collocation points

In 3D inversion, for both quadratic and cubic hydraulic head approximations, each element interface has one collocation point in the center of the interface (see Appendix A). Due to the harmonic

properties of these approximating functions, one collocation point can ensure that the average value of the functions is preserved across the element interface. In order for the solution of the direct method to satisfy the flow equation globally, a set of residual functions needs to be minimized at each collocation point p_j:

$$\int R(\Gamma_j)\delta(p_j-\varepsilon)d\Gamma_j = 0, \quad j=1,\ldots,m_c \tag{4}$$

where m_c is the total number of element interfaces, $R(\Gamma_j)$ is the residual of an approximating function on the jth interface, and $\delta(p_j - \varepsilon)$ is the Dirac delta weighting function. In 3D inversion, the Dirac delta weighting function needs to be chosen based on the size of the inversion matrix (see detail in Appendix B).

For the quadratic head approximation, when the element interface lies within a single hydrofacies zone, the residual equations enforcing head and flux continuity across each element interface are written for these 4 quantities: $\tilde{h}_q,\ \tilde{q}_{qx},\ \tilde{q}_{qy},\ \tilde{q}_{qz}$. However, when the interface links two elements of different hydraulic conductivities, only two residual equations are needed in order to honor the reflection principle: $\tilde{h}_q,\ \tilde{q}_{qn}$ where $\tilde{q}_{qn}$ represents the normal component of the elemental Darcy flux to the interface. For the cubic head approximation, the residual equations enforcing continuity of head, flux, and their derivatives across an element interface are written for 9 quantities: $\tilde{h}_c,\ \tilde{q}_{cx},\ \tilde{q}_{cy},\ \tilde{q}_{cz},\ \frac{\partial\tilde{q}_{cx}}{\partial y},\ \frac{\partial\tilde{q}_{cx}}{\partial z},\ \frac{\partial\tilde{q}_{cy}}{\partial z},\ \frac{\partial\tilde{q}_{cx}}{\partial x},\ \frac{\partial\tilde{q}_{cy}}{\partial y}$. Due to the linear dependency between the second order derivatives of the state variable (hydraulic head), $\frac{\partial\tilde{q}_{cz}}{\partial z}$ does not need to be evaluated (Galybin and Irsa, 2010). Similarly, when the interface is adjacent to elements with different conductivities, only 5 residual quantities are evaluated: $\tilde{h}_c,\ \tilde{q}_{cn},\ \frac{\partial\tilde{q}_{cn}}{\partial x},\ \frac{\partial\tilde{q}_{cn}}{\partial y},\ \frac{\partial\tilde{q}_{cn}}{\partial z}$.

In the following subsection, the equations are written for an interface which lies within a hydrofacies zone. For those that lie at the hydrofacies boundaries, the equations will be appropriately reduced (as discussed above) and are thus not presented. Moreover, Eq. (4) is also formulated at the observation locations, where $\delta(p_j - \varepsilon)$ now represents a weighting imposed due to measurement errors (δ is 1.0 if the observations are error-free), and $R(\Gamma_j)$ is replaced with the residuals at the data locations $R(t_j)$, where t_j is the jth observed data.

3.3. Algorithms

The algorithms of the 3D direct method are presented in this section, where the hydraulic head solution is first approximated with the quadratic formulation, and then with the cubic formulation.

3.3.1. Quadratic approximation

For the quadratic approximation, 4 continuity equations for the head and flux components are evaluated based on Eq. (4). At the jth collocation point $p_j(x_j, y_j, z_j)$ lying on an interface between elements (k) and (l), the following continuity equations can be written:

$$\begin{aligned}
\delta(p_j-\varepsilon)R_{h_q}(p_j) &= \delta(p_j-\varepsilon)\left(K\tilde{h}_q^{(k)}(x_j,y_j,z_j) - K\tilde{h}_q^{(l)}(x_j,y_j,z_j)\right) = 0\\
\delta(p_j-\varepsilon)R_{q_{qx}}(p_j) &= \delta(p_j-\varepsilon)\left(\tilde{q}_{qx}^{(k)}(x_j,y_j,z_j) - \tilde{q}_{qx}^{(l)}(x_j,y_j,z_j)\right) = 0\\
\delta(p_j-\varepsilon)R_{q_{qy}}(p_j) &= \delta(p_j-\varepsilon)\left(\tilde{q}_{qy}^{(k)}(x_j,y_j,z_j) - \tilde{q}_{qy}^{(l)}(x_j,y_j,z_j)\right) = 0\\
\delta(p_j-\varepsilon)R_{q_{qz}}(p_j) &= \delta(p_j-\varepsilon)\left(\tilde{q}_{qz}^{(k)}(x_j,y_j,z_j) - \tilde{q}_{qz}^{(l)}(x_j,y_j,z_j)\right) = 0
\end{aligned} \tag{5}$$

where the hydraulic head residual equation is multiplied by the hydraulic conductivity in order to extract the K value from the solution. By writing Eq. (5) at all the collocation points in the problem domain, a set of algebraic equations can be written with which head and flux continuity can be enforced locally within each element, while satisfying the global flow equation.

Eq. (4) is then written for the N observed hydraulic heads. For the kth element, where the tth observed head lies, we aim to minimize the difference between the observed head $h_t(x_t,y_t,z_t)$ and the approximating function at the same location: $\tilde{h}_{q/c}^{(k)}(x_t,y_t,z_t)$. This equation is also multiplied by K, and taking into account the observation weight $\delta(p_j - \varepsilon)$, we write a head measurement residual equation at the location of the observed head:

$$\delta(p_t-\varepsilon)\left(K\tilde{h}_{q/c}^{(k)}(x_t,y_t,z_t) - Kh_t(x_t,y_t,z_t)\right) = 0, \quad t=1,\ldots,N \tag{6}$$

The right hand sides of Eqs. (5) and (6) are all zeros, thus the solution at this point would be trivial. At least one flux or flow rate measurement is needed for the inversion to succeed, which also reflects the well-known fact that hydraulic conductivity cannot be uniquely determined from the hydraulic head data alone (Hill and Tiedeman, 2007). For example, if an observed flux component (e.g., q_x) is available, Eq. (6) can be rewritten to create a flux measurement residual equation using the same error-based weighting scheme as that of the head observations:

$$\delta(p_t-\varepsilon)\left(\widetilde{q}_{x\,q/c}^{(k)}(x_t,y_t,z_t) - q_x(x_t,y_t,z_t)\right) = 0 \tag{7}$$

Similar equations can be written if additional flux components are measured. Alternatively, a flow rate measurement can be used. Because the flux approximating functions are given analytically throughout the problem domain, an approximating function of flow rate along any line or surface can be created by integrating the appropriate fluxes. For instance, in a unit cube with dimensions [0,0,0] to [1,1,1], a flow rate $\widetilde{Q}_x$ along one side of the model domain ($x = 1$) can be evaluated as a surface integral:

$$\widetilde{Q}_x(x,y,z) = \sum_{k=e}^{f}\left[\int_0^{dz^{(k)}}\int_0^{dy^{(k)}} \tilde{q}_{qx}^{(k)}dydz\right]$$

where $dy^{(k)}$ and $dz^{(k)}$ are the lengths of the kth element along the y and z axis, respectively, e to f represent a set of elements lying on the side of the domain at $x = 1$. Given an observed flow rate measured on the same surface (Qx), the flow rate measurement residual equation takes the form:

$$\delta(p-\varepsilon)\widetilde{Q}_x(x,y,z) = \delta(p-\varepsilon)Q_x \tag{8}$$

The addition of Eqs. (7) or (8) yields a non-trivial solution, which leads to the unique estimation of the hydraulic conductivities. The final equation system consists of Eqs. (5)–(8), which can be solved with a least-squares method (more explanation is provided later). Note that if flux and flow rate measurements are both available, Eqs. (7) and (8) can both be used (the same can be said if multiple flux and flow rate measurements exist). However, as demonstrated in the Results section, a minimum of one flux component or one flow rate measurement suffices to provide a well-posed inverse solution even when multiple hydraulic conductivities are estimated.

3.3.2. Cubic approximation

Based on Eq. (4), the cubic approximation of the hydraulic head leads to 9 continuity equations: hydraulic head, three Darcy flux components, three cross derivatives, and two second order derivatives of the hydraulic head. For the jth collocation point $p_j(x_j, y_j, z_j)$ lying on an interface between elements (k) and (l), we have the following continuity equations:

$$\begin{aligned}
&\delta(p_j-\varepsilon)R_{h_c}(p_j)=\delta(p_j-\varepsilon)\left(K\tilde{h}_c^{(k)}(x_j,y_j,z_j)-K\tilde{h}_c^{(l)}(x_j,y_j,z_j)\right)=0\\
&\delta(p_j-\varepsilon)R_{qcx}(p_j)=\delta(p_j-\varepsilon)\left(\tilde{q}_{cx}^{(k)}(x_j,y_j,z_j)-\tilde{q}_{cx}^{(l)}(x_j,y_j,z_j)\right)=0\\
&\delta(p_j-\varepsilon)R_{qcy}(p_j)=\delta(p_j-\varepsilon)\left(\tilde{q}_{cy}^{(k)}(x_j,y_j,z_j)-\tilde{q}_{cy}^{(l)}(x_j,y_j,z_j)\right)=0\\
&\delta(p_j-\varepsilon)R_{qcz}(p_j)=\delta(p_j-\varepsilon)\left(\tilde{q}_{cz}^{(k)}(x_j,y_j,z_j)-\tilde{q}_{cz}^{(l)}(x_j,y_j,z_j)\right)=0\\
&\delta(p_j-\varepsilon)R_{\frac{\partial q_{cx}}{\partial y}}(p_j)=\delta(p_j-\varepsilon)\left(\frac{\partial\tilde{q}_{cx}^{(k)}}{\partial y}(x_j,y_j,z_j)-\frac{\partial\tilde{q}_{cx}^{(l)}}{\partial y}(x_j,y_j,z_j)\right)=0\\
&\delta(p_j-\varepsilon)R_{\frac{\partial q_{cx}}{\partial z}}(p_j)=\delta(p_j-\varepsilon)\left(\frac{\partial\tilde{q}_{cx}^{(k)}}{\partial z}(x_j,y_j,z_j)-\frac{\partial\tilde{q}_{cx}^{(l)}}{\partial z}(x_j,y_j,z_j)\right)=0\\
&\delta(p_j-\varepsilon)R_{\frac{\partial q_{cy}}{\partial z}}(p_j)=\delta(p_j-\varepsilon)\left(\frac{\partial\tilde{q}_{cy}^{(k)}}{\partial z}(x_j,y_j,z_j)-\frac{\partial\tilde{q}_{cy}^{(l)}}{\partial z}(x_j,y_j,z_j)\right)=0\\
&(p_j-\varepsilon)R_{\frac{\partial q_{cx}}{\partial x}}(p_j)=\delta(p_j-\varepsilon)\left(\frac{\partial\tilde{q}_{cx}^{(k)}}{\partial x}(x_j,y_j,z_j)-\frac{\partial\tilde{q}_{cx}^{(l)}}{\partial x}(x_j,y_j,z_j)\right)=0\\
&\delta(p_j-\varepsilon)R_{\frac{\partial q_{cy}}{\partial y}}(p_j)=\delta(p_j-\varepsilon)\left(\frac{\partial\tilde{q}_{cy}^{(k)}}{\partial y}(x_j,y_j,z_j)-\frac{\partial\tilde{q}_{cy}^{(l)}}{\partial y}(x_j,y_j,z_j)\right)=0
\end{aligned}\tag{9}$$

The head measurement residual equation is formulated similarly as Eq. (6), with the difference that the approximating hydraulic head function is cubic. Similarly, Eq. (7) or Eq. (8) is rewritten with $\tilde{q}_x$ or $\tilde{Q}_x$ evaluated using flux approximating functions that are derived from the cubic head.

For both the quadratic and cubic head approximating functions, the final systems of equations can be assembled into a matrix form:

$$\boldsymbol{Ax}\cong\boldsymbol{b}\tag{10}$$

where $\boldsymbol{A}$ is a sparse matrix ($r\times s$). r is the number of equations, and s is the number of unknowns. If the domain is discretized into n elements, the quadratic approximation yields $s=9n+1$, while $s=16n+1$ for the cubic approximation. The number of equations can be determined by $r=4m_c+N+g$ for quadratic approximation and $r=9m_c+N+g$ for cubic approximation, where N is the number of observed hydraulic heads, g is the number of flux or flow rate observations ($g\geqslant 1$), $\boldsymbol{x}$ is the solution vector of size s, $\boldsymbol{x}\in\{Ka_0^{(1)},\ldots,Ka_8^{(n)},K\}$ or $\boldsymbol{x}\in\{Ka_0^{(1)},\ldots,Ka_{15}^{(n)},K\}$, $\boldsymbol{b}$ is of size r, consisting of all zeros except g non-zero fluxes or flow rates. The system of equations can be solved using a least-squares minimization technique with either a direct solver (e.g., $x=(A^TA)^{-1}A^Tb$) or an iterative LSQR solver (Paige and Saunders, 1982). For the example problems presented in this study, in addition to observed heads, one flow rate or flux measurement was provided to inversion which was sufficient to uniquely determine one or more hydraulic conductivities.

4. Results

The inversion algorithms presented in Section 3 are tested on several synthetic examples where the true aquifer flow conditions were simulated with MODFLOW2000, from which a number of hydraulic heads, flow rate, or flux were sampled. For several test examples inverting a homogeneous aquifer, inversion results were obtained using both the quadratic and cubic head approximations with (mostly) error-free measurements. Increasing inverse grid densities were tested. An analysis was then conducted to evaluate the issues of data support, parameter sensitivity to observation density, and of when observation data can yield reliable K estimates. Finally, a problem with 4 conductivities was inverted under increasing head measurement errors. In this section, dimensions for all relevant quantities assume a consistent set of units (e.g., head in ft, K in ft/d, q in ft/d, Q is ft^3/d), thus units of the various quantities are often not labeled.

4.1. Convergence and accuracy of the direct formulations

In this subsection, two homogeneous forward models were created to test the inverse algorithm. For both models, a cubic domain of dimensions [0,0,0]–[1,1,1] was created. To each model, a true K value of 1.0 was assigned. A finite difference grid with $25\times25\times25$ block elements was used for the forward simulations, thus a theoretical maximum of 15,625 observed hydraulic heads can be extracted from each model (i.e., enough data exist for a sensitivity study using random selections of the observations). The only difference between the two models lies in how the aquifer boundary conditions were specified:

(1) A linear flow model or **Model1** (Fig. 2). The BC were specified as: $h=1000$ is assigned to the top boundary and 100 is assigned to the bottom boundary, while the sides have no-flow boundaries. Under this set of BC, the FDM solution of hydraulic heads and streamlines for $K=1$ is shown (Fig. 2). A vertical flow rate (Q_z) was sampled from this solution along the model side boundary at $x=1$. Given these BC, this measured flow rate is considered error-free.
(2) A nonlinear flow model or **Model2** (Fig. 3). The BC were specified as: the top boundary has a hydraulic head following a parabolic function $(300+100[(x+0.3)^2+(y+0.4)^2])$, while the remaining 5 sides were assigned no-flow bound-

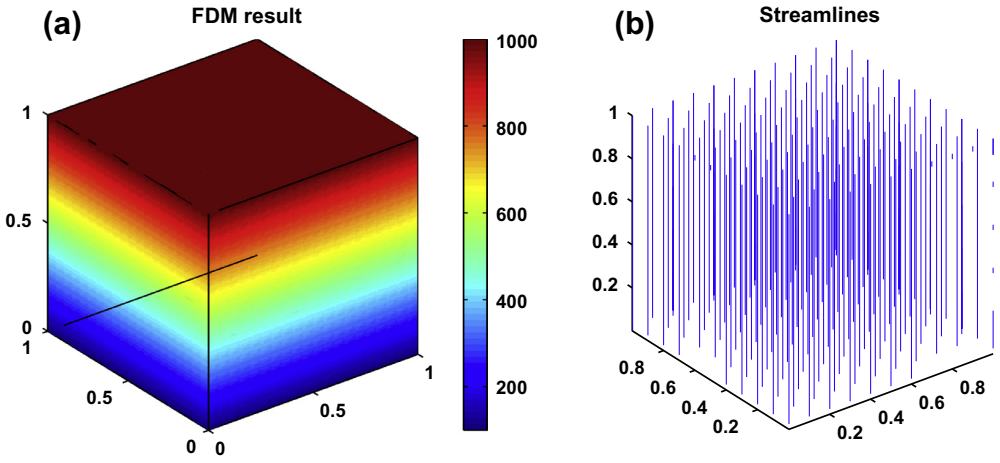

Fig. 2. Linear flow model, or **Model1**. FDM true solution of heads (a) and streamlines (b).

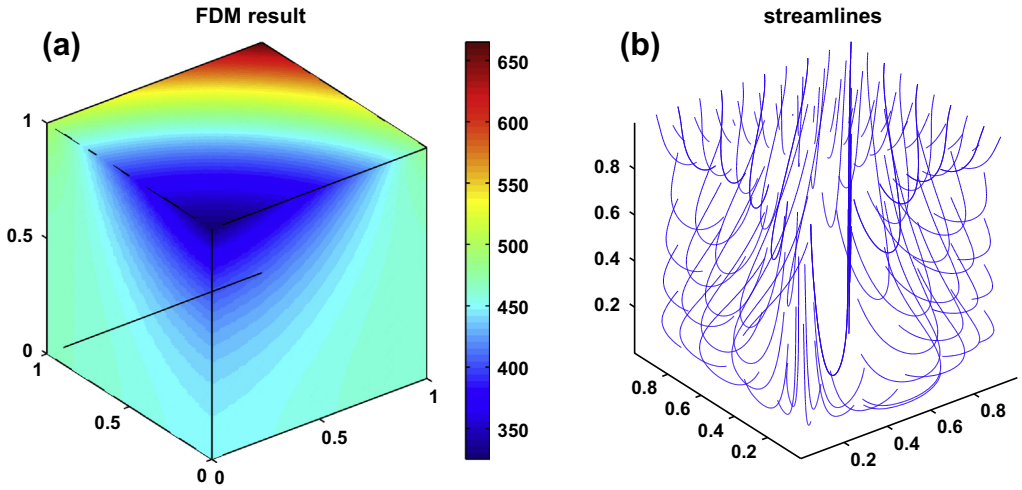

Fig. 3. Nonlinear flow model, or **Model2**. FDM true solution of heads (a) and streamlines (b).

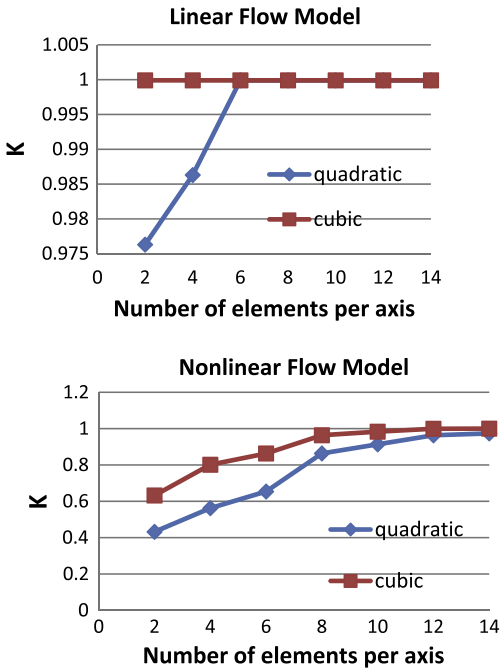

Fig. 4. Grid refinement study for **Mode1** and **Model2**, based on 50 observed heads and one observed flow rate. When the number of elements per axis is 2, the inverse grid is $2 \times 2 \times 2$, and so forth.

aries. Under this set of BC, the FDM solution of hydraulic heads and streamlines for $K = 1$ is shown (Fig. 3). A flow rate, Q_z, was sampled along the model side boundary at $x = 1$. A measurement error of +3% was imposed on this flow rate.

From each forward model, besides the one flow rate measurement, fifty heads were sampled in a quasi-regular fashion, without imposing any measurement errors. These data were used as the observed data for inversion where both the quadratic and cubic head approximating functions were tested. Under both linear (**Model1**) and strongly nonlinear flow (**Model2**), a convergence analysis was conducted whereby the inverse grid was increasingly refined. Results of this grid refinement study are provided in Fig. 4, which demonstrates the applicability of the 3D inversion formulations. For the given observed data, inversion accuracy increases with grid refinement. For a fixed grid, however, the cubic head formulation leads to more accurate K estimates compared to the quadratic head formulation. In other words, the cubic formulation achieves similar accuracy as the quadratic formulation but with fewer elements (in the following analysis, all inversions were done using the cubic formulation). Moreover, flow condition also influences the accuracy of inversion: under linear flow, both formulations converge to the true K quickly (cubic at $2 \times 2 \times 2$; quadratic at $6 \times 6 \times 6$); under nonlinear flow, both converge more slowly and a higher resolution grid is needed to achieve the same level of estimation accuracy. Because with the larger grid sizes, the inversion takes longer time, a $6 \times 6 \times 6$ grid is used in all subsequent analysis with the exception of the last example (Section 4.4). This discretization allows us to conduct a sensitivity study with relative efficiency.

4.2. Data support

The answer to "How many observations do we need to be able to estimate all the unknown parameters?" depends on the problem of interest. In heterogeneous aquifers, the number of observations is rarely sufficient to provide perfect (high resolution) solutions (Moore and Doherty, 2006). However, given a hydrofacies parameterization, there usually exists a threshold level of measurement data that can lead to satisfactory estimation of the parameters and, in our case, the boundary conditions as well. Because the direct method invokes an efficient one-step solution procedure, it is highly suitable as an analysis tool to understand the issue of data support. For both **Model1** and **Model2**, observed heads were randomly sampled to provide the input data for inversion, keeping the same flow rate measurement along the model side boundary at $x = 1$. For a given data support (N varies from 2 to 100), heads were randomly sampled from the FDM 102 times. $N = \{2, 3, 4, 5, 10, 20\}$ for **Model1**; $N = \{5, 10, 15, 20, 25, 30, 40, 50, 100\}$ for **Model2**. For both models, the estimated K was plotted against the data support, N (Figs. 5 and 6). At each N, 102 inverse solutions were obtained which result in the following estimated K values: minimum, maximum, 80% percentile (box), and median (connected solid line).

For both models, conductivity converges to the correct value ($K = 1$) with increasing data support, as expected. With the exception of $N = 2$ (**Model1**) and $N < 20$ (**Model2**), the estimated K generally varies within one order of magnitude from the true value, i.e., the estimated K is greater than 0.1 and less than 1.5. For each model, there appears to be an approximate threshold N value where the

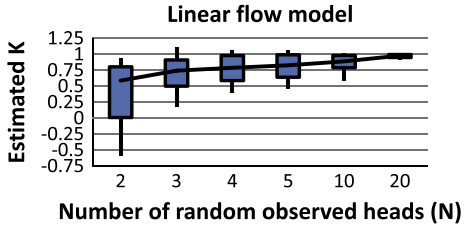

Fig. 5. Conductivity estimated for **Model1** when increasing number of the observed heads are provided to inversion. The true K of the problem is 1.

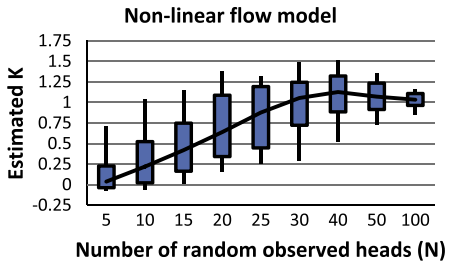

Fig. 6. Conductivity estimated for **Model2** when increasing number of the observed heads are provided to inversion. The true K of the problem is 1. The one observed flow rate contains a +3% measurement error.

estimated K stabilizes and the variance of the K starts to decrease: $N = 5$ (**Model1**), $N = 30$ (**Model2**). For **Model1**, 80% of the estimated K ranges from 0.64 to 1.0 when $N = 5$; for **Model2**, this envelop is from 0.7 to 1.25 when $N = 30$. At these support sizes, adding more observed heads does not significantly increase the accuracy and reliability (i.e., reduction in the estimation variance) of the result. This behavior was observed in other studies as well and was referred to as a 'screening effect' (Feyen et al., 2003). The variance is also larger when the number of the observations is small. An exception is that when N is very small (e.g., 2 for **Model1** and 5 for **Model2**), a few estimated conductivities actually become negative due to incorrect estimation of the hydraulic head gradient $[\partial h/\partial x, \partial h/\partial y, \partial h/\partial z]^T$. In these cases, wrong gradient signs can be computed locally from the few observed heads that are spaced either too close to one another or sampled at locations that make gradient evaluations difficult, e.g., $\partial h/\partial z$ is estimated using measured heads that are sampled on or near a horizontal plane. In these cases, inspection of the reconstructed streamlines (not shown) reveals incorrect local flow directions, indicating the issue with gradient estimation. Clearly, when data are sparse, head gradient estimation becomes challenging in 3D and inversion accuracy suffers accordingly. This problem vanishes when more observed heads are provided to inversion with which head gradient vectors can be more accurately computed. In a field situation, before any inversion is carried out, the existing measurements need to be closely examined to evaluate whether head gradient, which varies with space, can be accurately determined. Without such data, inversion accuracy will be poor regardless of the inverse method used. Moreover, even when N is very small, the degeneracy in the head gradient estimation (i.e., negative K estimates) occurs in only about 10% of the inverse solutions, while 80% of the estimated K still remains positive.

The K estimation variance, together with the evolution of its median value, suggests a minimum number of head observations for the inversion to succeed under linear and nonlinear flow. For **Model1** (linear flow), if a 10% conductivity estimation error is considered acceptable, 10 observed heads (along with the one observed flow rate) are sufficient to provide an accurate K estimate. Upon inspecting the solutions, the highest errors in K estimation tend to occur when the observed heads lie close to one another (i.e., average distance <0.5), resulting in a strong screening effect. In these cases, model domains extend beyond the observation locations, leading to extrapolation in the rest of the model where the observed data do not exist. In these outer regions, continuity of head and flux are imposed but locally these solutions are not conditioned to measurements, which leads to a greater overall estimation error. In real applications, model domain is typically defined by the observation locations (see Section 2). Thus, should the model domain be selected to more closely follow the data, the inversion accuracy is also expected to improve. For **Model2** (nonlinear flow), given the same acceptable error in K estimation, an N threshold appears around 40. Interestingly, accurate result can also be obtained with an N as low as 10, i.e., near the maximum estimated K. This particular solution suggests that for $N = 10$, an optimal distribution of the observed heads exists. These heads may be described as a set of "influential observations with high information content" for the K estimation (Hill and Tiedeman, 2007). Together, these results suggest that the accuracy of K estimation depends not only on the quantity of the observations but also on their locations. Furthermore, when N is greater than 30, the median K is generally overestimated due to the imposed +3% error on the observed flow rate. However, when N increases from 30, the influence of this flow rate error on K estimation becomes less pronounced: when $N = 100$, only around +3% overestimation of the median K is observed.

4.3. Information content of the observations

Various sensitivity analysis methods exist with which the influence of observations on parameter estimation can be assessed. These methods are often based on estimating a sensitivity matrix by differentiating the observations with respect to the parameters (Hill and Tiedeman, 2007). Here, the fit-independent Composite Scaled Sensitivity (CSS) statistic is tested, which provides a scalar value summarizing the total information provided by all observations for the estimation of one parameter, in our case, K of the aquifer:

$$\mathrm{CSS} = \sum_{j=1}^{N+1}\left[\frac{\mathrm{DSS}_j^2}{N+1}\right]^{0.5}, \quad \mathrm{DSS}_j = \left(\frac{\partial h_j}{\partial K}\right)|K| \tag{11}$$

where N is the number of head observations and (+1) reflects the one flow rate measurement. Here, for a subset of the support sizes: $N = \{5, 10, 20, 40, 100\}$, CSS is computed for **Model2** using the forward model for each set of the (randomly sampled) observed heads at their measurement locations. (Note that for each support size, 102 inversion runs had been carried out with which K was estimated given the same observed heads.) The CSS values are plotted against the absolute error of K estimation (Fig. 7). Larger N leads to higher CSS, indicating an overall increase of the information content of the data, which then leads to a better estimated K. For a given dataset, however, a slight increase in the K estimation error is observed with increasing CSS. It suggests that for this model, CSS is not able to give detailed information to distinguish if a given set of the observations can result in an accurate and reliable K estimate. Similar to Fig. 6, we observed that $N \sim 40$ appears to be a measurement threshold: when $N > 40$, the K estimation error decreases sharply with increasing CSS.

For **Model2**, CSS appears to be an inadequate indicator of the information content of the data, i.e., whether a particular set of the observations can yield accurate inversion results. Here, we present a simple and efficient OAT (one-observation-at-a-time) procedure which is shown for limited test cases to be a good indicator of whether a set of observations can lead to a reliable K estimate. In this procedure, we propose to solve the inverse

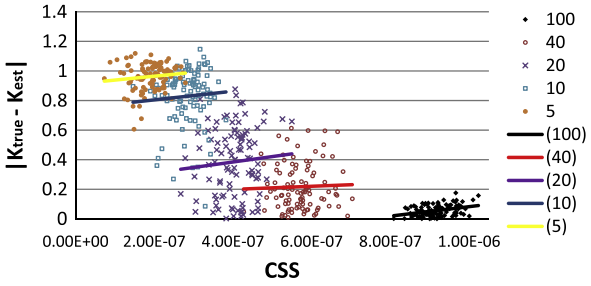

Fig. 7. Computed CSS for **Model2** when an increasing number of the observed heads is provided to inversion. For each observation set (of size N), 102 inversion runs were carried out. Thick lines represent a linear fit of the K estimation error against CSS for a particular observation set.

problem using only 1 observed head at first, recording the estimated conductivity value, i.e., K_1. Then, one more observed head is added, yielding K_2, and so on until K_N (N represents the total number of the observed heads in the dataset). We then evaluate the convergence behavior of the estimated K versus the number of observations used. If K appears to converge (i.e., the estimated K appears to stabilize when increasing number of the head measurements are used), then we randomize the sequence of the head selections *from the same observation dataset*, and repeat the analysis to obtain a new set of K_1 to K_N. Again, the behavior of K is inspected and compared to the first sequence. This analysis can be repeated many times, and all sequences of K are compared together. The estimated K using the full dataset (of size N) is considered reliable if all the K sequences appear to converge after certain measurement threshold is reached.

To illustrate the OAT procedure, 3 examples using **Model2** are presented with $N = 50$ (again, only one flow rate measurement is used). In each example, 50 heads were randomly sampled at different locations, yielding 3 alternative measurement datasets. For each measurement set, 4 randomized sequences were created using the OAT procedure. Three different behaviors are observed: (1) Fast convergence (Fig. 8a): for all 4 sequences, a stable K is obtained with as few as 30 observed heads. After 30, adding more observed heads does not change the result, but may increase the reliability of the estimated K. In this case, the particular measurement set (a total of 50 heads) can provide enough information for the reliable K estimation. (2) Slow convergence (Fig. 8b): a stable K is obtained at 44 observed heads. In this case, the measurement dataset (another randomly selected 50 heads) may provide less information for reliable K estimation. (3) Non-convergence (Fig. 8c): none of the sequences suggest that the estimated K is stabilizing. In this case, the measurement dataset (yet another 50 heads) does not provide sufficient information for reliable K estimation, thus more observation data would be needed. In the above analysis, a few sequences first appear to converge, but switch to very different K values as more observed heads are added, e.g., the sequence labeled "3_1" in Fig. 8b, when N reaches 15. This suggests that the addition of one more observed head leads to a significant change in the inverted flow field, thus illustrating the non-uniqueness issue discussed in Irsa and Zhang (2012), where different BC associated with different flow patterns can all satisfy the same observed data. This behavior also suggests the necessity of randomizing the sequence when carrying out the OAT analysis. Having multiple sequences can help identify possible false convergence behavior.

To evaluate the accuracy of BC recovery, the BC obtained from one inverse solution (**Model2**: dataset "2" when $N = 50$; see Fig. 8a) are compared with the true BC which were used in the forward FDM to generate the observation data. Along a diagonal profile on the model top boundary where the true hydraulic head was

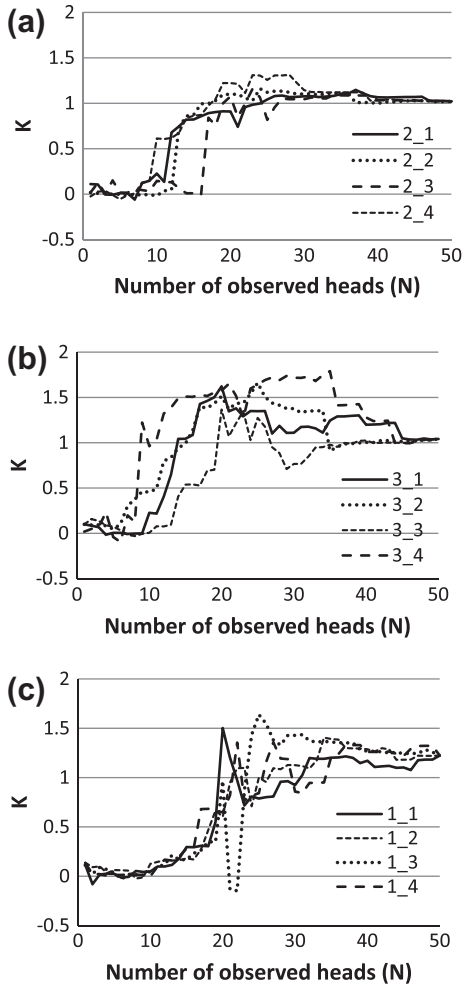

Fig. 8. OAT test runs for 3 different measurement datasets, with (a) fast converging, (b) slow converging, and (c) non-converging characteristics. For each dataset, 4 randomized sequences were run. True K of this problem is 1.

specified as a parabolic function, the recovered head profile closely matches the true head profile (Fig. 9a). In addition, a separate inversion is carried out when the model domain contains two horizontal hydrofacies zones of equal thickness (the bottom hydrofacies K is 100 times the top hydrofacies K). The true model in this case is driven with a set of linear flow BC, thus flow is from top to bottom (this problem is similar to the heterogeneous problem described in the next section and is thus not presented in great detail). Along a straight line in the center of the model domain extending from the bottom boundary to the top boundary, the recovered head profile is again favorably compared with the true head profile (Fig. 9b). In all other inversion runs when accurate Ks were estimated based on a sufficient set of observation data, a similar accuracy in BC recovery is observed. Similar to K estimation, the accuracy in BC recovery also increases with the increasing number of the observation data.

4.4. Heterogeneous inversion and stability

A heterogeneous model is inverted where four hydrofacies zones exist within a computation domain of $x \in [0,100]$, $y \in [0,100]$, $z \in [0,100]$ (all units are in ft). In this analysis, the cubic hydraulic head formulation is used. At the hydrofacies interfaces where K differs across the neighboring elements, fewer equations are needed in formulating Eq. (9), as only the hydraulic head,

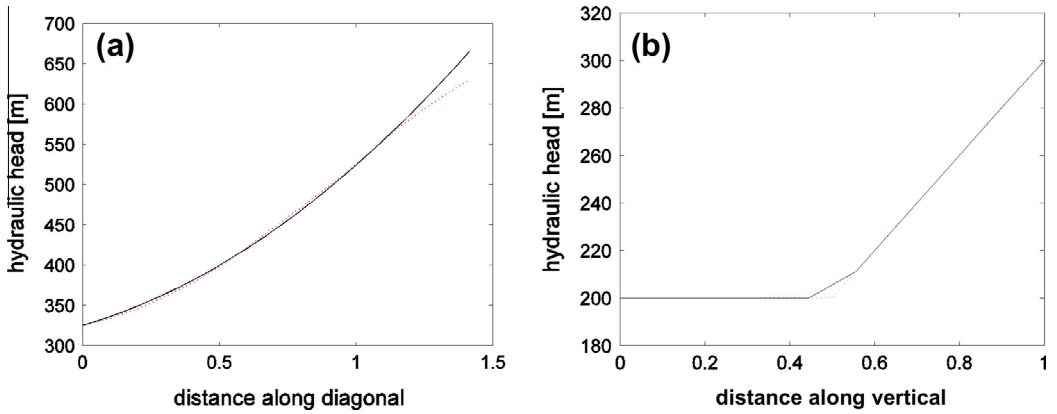

Fig. 9. Recovered hydraulic head profile (dotted line) compared to the corresponding true head profile (solid line) (a) along a diagonal line at the model top boundary in **Model2**, dataset "2", $N = 50$. (b) along the model center for a problem with two horizontal hydrofacies and linear flow boundary conditions.

Table 2
Estimated hydraulic conductivities (ft/d) when inversion is conditioned to observed heads with increasing measurement errors. Conductivities of the true model are also listed. The measurement error is defined by a percent of the total head variation in the solution domain. The computation time is obtained by running the inversion code on a dual-core 64-bit PC workstation.

	Hydraulic conductivities				Grid	Computation time (s)
	$K1$	$K2$	$K3$	$K4$		
True model	1.0×10^{-2}	5.0×10^{-2}	1.0×10^{-1}	5.0×10^{-1}	$50 \times 50 \times 20$	~5
Inversion: 0% (0)	1.0×10^{-2}	5.0×10^{-2}	1.0×10^{-1}	5.0×10^{-1}	$2 \times 2 \times 2$	~1
Inversion: ±0.1% (±0.1 ft)	9.7×10^{-3}	4.9×10^{-2}	9.7×10^{-2}	4.9×10^{-1}	$2 \times 2 \times 2$	~1
Inversion: ±0.5% (±0.5 ft)	5.7×10^{-3}	2.9×10^{-2}	5.7×10^{-2}	2.9×10^{-1}	$2 \times 2 \times 2$	~1
Inversion: ±0.1% (±0.1 ft)	1.01×10^{-2}	5.05×10^{-2}	1.01×10^{-1}	5.05×10^{-1}	$4 \times 4 \times 4$	~2
Inversion: ±0.5% (±0.5 ft)	1.08×10^{-2}	5.4×10^{-2}	1.08×10^{-1}	5.4×10^{-1}	$4 \times 4 \times 4$	~2

the normal flux, and its derivative are written for the continuity equations. Spatially, the 4 hydrofacies are organized as (the value of their respective hydraulic conductivity is given in Table 2):

- $K1$ zone: $x \in [0,50]$, $y \in [0,50]$, $z \in [0,100]$,
- $K2$ zone: $x \in [50,100]$, $y \in [0,50]$, $z \in [0,100]$,
- $K3$ zone: $x \in [0,50]$, $y \in [50,100]$, $z \in [0,100]$,
- $K4$ zone: $x \in [50,100]$, $y \in [50,100]$, $z \in [0,100]$.

Under a set of true model BC (specified head of 200 ft and 100 ft for the top and bottom boundaries, respectively, and no-flow for the sides), a forward FDM is simulated with a dense grid of $50 \times 50 \times 20$ from which a set of observation data are sampled. These data consist of 64 randomly sampled heads and one vertical Darcy flux component (q_z) sampled at (83.0, 83.0, 82.5). The inversion is carried out first with a coarse grid, and then with a refined grid. Initially, error-free measurements are used, and the estimated conductivities are identical with those of the true model (Table 2). Then, increasingly higher measurement errors are imposed on the observed heads while keeping the mean error approximately zero (error is not imposed on the flux measurement). For example, if the errors is ±0.1%, it means that we randomly add or subtract 0.1% of the total head variation to each measured head sampled from the true model. Tapes and pressure transducers can yield head measurements with a precision of less than 1 cm (Post and von Asmuth, 2013). Pressure transducers sometimes suffer from environmental effects, which can lead to head measurement errors on the order of several cm or even decimeters (Post and von Asmuth, 2013). In comparison, our head errors of ±0.1–±0.5 ft (±3–±15 cm) are reasonable. Though other techniques can lead to even greater head measurement errors (e.g., meters), Post and von Asmuth (2013) recommends that "the use of such data beyond anything other than an initial, general reconnaissance study is questionable, and any quantitative analysis based on them should be avoided". Therefore, we did not test head errors greater than ±0.5 ft.

When a small inverse grid ($2 \times 2 \times 2$) is first used, the estimated conductivities become less accurate with increasing head measurement errors, although the inversion results are still stable, i.e., for the given error magnitudes, the estimated hydraulic conductivities do not vary from the true values by more than one orders of magnitude. When the inverse grid is refined to $4 \times 4 \times 4$, for the same measurement errors, much improved K estimates were obtained, especially for the case with the larger measurement errors (±0.5 ft). Clearly, similar to the homogeneous problems inverted earlier, inversion accuracy of the heterogeneous problem is also affected by grid resolution. The conductivity estimation error, however, is expected to grow when the measurement errors are further increased and/or when the number of observed heads is further decreased (this latter problem was evaluated previously with the homogeneous problems and will not be repeated here). A systematic study is needed, however, to evaluate an optimal monitoring network with which the inversion can be carried out with a high degree of stability – i.e., accurate parameter estimates that are robust to measurement errors while only a limited number of head measurements is provided to inversion.

The recovered head boundary conditions are very accurate when error-free data are used to condition the inversion (not shown), but become less accurate when the measurement error is increased. These results are consistent with what was found in our earlier 2D studies. Computation time for the above inversion (i.e., a program written with MATLAB 2012a) is extremely fast when a least-squares direct matrix solver is used. Generally, it takes less than two seconds for the solver to converge, and the

solution time does not appear to be affected by the increasing measurement errors that are tested in this problem. However, for 3D inversion with much larger grid sizes, the system of equations will become much bigger. Iterative solution techniques will likely be needed for which a number of efficient LSQR solvers (both serial and parallel) are under development (Lee et al., 2013).

5. Discussion

Using synthetic examples providing a set of true models from which measurements can be sampled, this study demonstrates the applicability of the new direct method for aquifer inversion in three dimensions. In formulating the fundamental solutions of inversion, earlier studies evaluated a set of lower order approximating functions, which were shown to provide sufficiently accurate solutions for different 2D problems (Irsa and Zhang, 2012; Wang et al., 2013). For 3D inversion, two sets of approximating functions of increasing complexity are developed and tested: quadratic head and linear Darcy flux versus cubic head and quadratic Darcy flux. Although the lower order approximating functions can yield accurate results when the inverse grid is refined, the higher order approximating functions can lead to a faster convergence of the estimated conductivity at a lower level of grid discretization. Regardless of the order of approximation, the direct method can yield accurate results given a sufficiently refined grid, whereas high accuracy can be gained with a coarse grid using higher approximation. Although a tradeoff exists between the order of approximation and the number of inverse grid cells, the inverse analysis can be performed with a high computational efficiency. Moreover, based on two simulations with identical parameterization but with different flow fields (uniform versus strongly nonuniform), the effect of boundary conditions, or the degree of flow tortuosity, also impacts the inversion accuracy. The cubic approximating function is found to be more robust when different flows are inverted, and is thus chosen for the majority of the analysis. A sensitivity analysis is then conducted to elucidate the effect of sampling density on the inversion accuracy. The results suggest that the location of the measurement data can also influence inversion: when the measured heads are clustered, the inversion accuracy suffers because of a greater extrapolation error. An OAT procedure is used to determine if a given set of measurements can lead to a reliable K estimate. Because the direct method is computationally efficient, a large number of inversion runs, as required by the OAT procedure, can be completed quickly. The optimal measurement location, however, remains undetermined and will require additional analysis for which a global sensitivity technique will likely be needed (Saltelli et al., 2008). Finally, using a problem with four hydrofacies, stability of inversion under increasing observation errors is demonstrated. The inversion accuracy is not only influenced by the magnitude of the measurement errors but is also affected by the inverse grid resolution.

In conducting the above analyses, which were carried out to analyze the inverse algorithm and its stability, the observation data include hydraulic heads and a single subsurface flow rate, or hydraulic heads and a single Darcy flux component. Clearly, to apply the direct method to inverting problems under non-pumping conditions, an issue exists with measuring the subsurface groundwater fluxes or flow rates which are needed for inversion. One way to collect flux measurements is to conduct borehole flowmeter tests (Molz et al., 1994) or downhole flow logging (Gellasch et al., 2013) under ambient flow. To measure subsurface flow rates, hydrograph separation can be utilized, although this technique requires that aquifer intersect streams whose gain/loss can be accurately measured. In studying groundwater–surface water interactions, various seepage meters can directly measure water fluxes at sediment–water interfaces (Kalbus et al., 2006). Indirect approach can use Darcy's Law to infer subsurface fluxes based on local K and hydraulic head measurements. For example, using the Multilevel Slug Test, a local K can be estimated at each packed-off interval (Butler, 2005). Before the test (under ambient flow), if the same interval is subject to multiple head measurements at locations above and beneath this interval, an in situ groundwater flux can be inferred. In addition, new measurement techniques for in situ groundwater flux determination are now available (Labaky et al., 2009). With the Point Velocity Probe, for example, both the magnitude and direction of the average linear velocity can be measured. If porosity measurement is also available, Darcy flux vectors can then be determined. The above discussion suggests that subsurface flow rate or flux measurements can in theory be obtained if the appropriate tests are conducted. However, some of these fluxes are indirect measurements (e.g., those determined by Distributed Temperature Sensing involve inverse modeling of the measured temperatures), and the associated measurement errors may be higher. In addition, under the Dupuit–Forchheimer condition, new inverse formulation has been developed to account for source/sink effects (e.g., pumping and recharge) (Zhang, submitted for publication). For problems with heterogeneous conductivity and recharge distributions, inversion is successful given a single pumping rate in addition to hydraulic heads as measurements. For these problems, *subsurface* flux or flow rate observations are no longer needed. The extension of the 3D method to address source/sink effects will be investigated in the future. To summarize, data requirement of the new inverse method is not unreasonably high. The potential of this method to be adopted by real world analysis can be enhanced by new measurement techniques or improved formulations.

A fundamental contribution of our series of studies is to prove, via the direct method, that boundary condition information is not needed for estimating aquifer parameters including hydraulic conductivities (and source/sink rates). With the objective-function-based approaches, hydraulic head and flux BC must be specified along the entire model boundaries, because these methods require the repeated simulations of a forward flow model in order to minimize the objective function. One issue with these approaches lies in the fact that BC are typically unknown in real aquifers, and if a wrong set of BC is assumed, parameters estimated using objective functions are likely non-unique. As demonstrated in Irsa and Zhang (2012), two different sets of BC can give rise to two different flow fields both of which can perfectly fit the same observed data, yielding a zero objective function. Moreover, when BC are specified to the forward model, these traditional methods in effect require that inversion be conditioned to these boundary heads or fluxes. *In other words, by specifying BC to a forward model in order to minimize an objective function, the calibrated model is "fitted" to these heads or fluxes*. The problem is that such heads or fluxes are not real measurements that are sampled from the aquifer; rather they reflect a conceptual assumption made by the modeler. Because of subsurface uncertainty, if a wrong BC assumption is made (e.g., leakage exists along a presumed no-flux boundary), this will result in the so-called "model error" which is difficult to remediate using the objective functions, e.g., various authors have discussed how the objective functions may be modified to account for such errors (Doherty and Welter, 2010). As demonstrated in Section 2 of this study, even in the extreme case where boundary heads are sampled everywhere in order to provide the BC for the forward model, measurement errors, which effectively create a large number of "incorrect measurements" along these boundaries, can significantly impact the accuracy of inversion using the objective function. With the direct method, the heads, fluxes, or flow rates are provided to inversion *at the locations where they are measured*, and they can be anywhere inside the model domain or on the

model boundaries. Compared to the traditional methods, no assumptions about the BC are made, eliminating the possibility of making the type of "model errors" that can arise due to a wrong BC assumption. In fact, our series of studies demonstrate that observation data that are sampled anywhere in the solution domain (with a minimum of one flux or one flow rate measurement) can effectively replace the need for specifying the BC along the entire model boundaries.

Although BC can in theory be calibrated, such an approach is likely inefficient. This is because infinite combinations of parameters and BC can satisfy the same observed data and non-uniqueness in calibrating the model parameters and model BC can only be eliminated at the limit where the observed data are sampled everywhere. In the real world, both the location of the aquifer boundaries and their boundary conditions are typically uncertain. As demonstrated in Section 2, the direct method applies to problems when the location of the aquifer boundaries is unknown, in which case the inversion domain is defined by the location of the measurements. This is again because the direct method does not built a forward model to evaluate objective functions. A further issue with the objective-function-based methods is computation efficiency. For example, using global optimization techniques (i.e., genetic algorithm, neural net, and others), thousands or more forward models must be solved to minimize an objective function (and if BC are additionally calibrated, more forward problems must be solved). With the direct method, given appropriate measurements, both the parameters and the unknown model BC can be simultaneously estimated. It is computationally efficient because the inversion only involves a single matrix solve. If appropriate approximating functions are used, the inverse grid can also be very small, leading to high computation efficiency. An exception is when the inverse method is combined with geostatistics, whereas many parameter realizations are inverted to account for the uncertainty in hydrofacies distribution (Wang et al., 2013). Integration of the 3D method with geostatistics will be addressed in the future.

6. Conclusion

In this study, a direct inverse method is presented for three-dimensional steady-state aquifer inversion where the aquifer boundary conditions are unknown. This method extends the two-dimensional study of Irsa and Zhang (2012), where its key strength lies in its computational efficiency. The formulation of the inverse method is based on (1) creating local solutions, or approximating functions, of hydraulic head and Darcy flux that satisfy the homogeneous, local flow equation; (2) enforcing the continuity of head and flux globally via a set of collocation points that lie on elemental interfaces; (3) conditioning the local solutions at the measurement locations. Because of this formulation, there is no need to fit an objective function, nor is there a need for repeated simulations of the forward flow model. Via step (3), the noisy observed data can be directly incorporated into the solution matrix, which is solved in a one-step procedure. The inversion results include hydraulic conductivities and head and flux approximating functions from which the model boundary conditions can be inferred.

Two hydraulic head approximating functions were tested, one employing quadratic approximation of the hydraulic head, the other cubic approximation. Compared to the quadratic approximating function, the cubic function leads to a faster convergence of the estimated hydraulic conductivity at a lower level of grid discretization, while it is also more robust when different flow conditions are inverted. Two different boundary conditions were also tested, one leading to linear flow, the other strongly nonlinear flow. Under both boundary conditions, the estimated conductivities converge to the true values with the refinement of the inverse grid, and the inversion results were shown to be accurate when a sufficient number of the observation data were used. Under linear flow, for example, 10 observed heads and 1 observed flow rate measurement can lead to accurate inverse solutions. Under nonlinear flow, however, 40 observed heads and 1 flow rate measurement are needed. Inversion is also successful using observation data such as 64 hydraulic heads and a single Darcy flux component. This level of data requirement is considered quite high if traditional water wells are used for the hydraulic head measurements. On the other hand, multilevel sampling wells can provide the much needed vertical resolution to obtain the measured heads in three-dimensions. These new technologies can significantly reduce the number of observation wells needed for the inversion to succeed. Moreover, the observed heads are randomly sampled, although measurement location is known to be a significant factor that can impact the accuracy of parameter estimation (Hill and Tiedeman, 2007). Based on the insights of this study, future work will explore optimal sampling locations, thus data requirement for inversion can be further reduced. Furthermore, to understand data worth, a sensitivity analysis is conducted whereby the inversion accuracy is evaluated when increasing observed heads are sampled. The results of this analysis are analyzed first with the composite scale sensitivity (CSS) which can reveal the overall information content of the data. The more heads are sampled, the higher the CSS, and the more accurate the inverse solution. However, when the number of measurements is fixed, CSS cannot identify whether a particular set of the observations can lead to a reliable conductivity estimate. A one-observation-at-a-time (OAT) approach is proposed, which can identify the reliability of the estimated conductivity for a given set of the observations. To evaluate the stability of the inverse method when measurement data contain errors, a problem with 4 hydrofacies zones is inverted. The results are accurate when the measurement error is small but become slightly less accurate when the error is larger. In summary, flow condition, inverse formulation, grid discretization, observation data density and location, and measurement errors can all influence the accuracy of inversion.

This study points to an efficient way of conducting first-pass, low-cost aquifer characterization where both aquifer parameters and aquifer boundary conditions can be obtained from limited site data, prior to conducting pumping tests or other aquifer stimulation techniques. In particular, Section 2 suggests that the new method can act as a low-resolution screening model to infer the unknown site BC, which when given to PEST or other objective-function-based techniques, may improve their results. Base on the insights of this study (e.g., more measurements are needed to successfully invert nonlinear flow), future studies will investigate sensitivity measures that take into account the aquifer flow condition, which can then help identify a set of optimal observation locations. Future work will also incorporate site geostatistical data in three-dimensions to account for realistic aquifer heterogeneity and to explicitly quantify uncertainty in both parameters and boundary conditions. Joint hydrological and geophysical inversion is of interest, whereby geophysical measurements correlated to the hydrological parameters can be used to provide additional constraint questions. By adding such equations to inversion, highly parameterized techniques estimating a greater number of parameters (e.g., K at each grid cell) will be attempted.

Acknowledgement

The authors wish to acknowledge the Center for Fundamental of Subsurface Flow at the School of Energy Resources at the Univer-

sity of Wyoming (WYDEQ49811ZHNG) and NSF CI-WATER (Cyberinfrastructure to Advance High Performance Water Resource Modeling) for the support. Thoughtful comments from two anonymous reviewers helped improve the breadth and depth of the current work.

Appendix A. Number of collocation points per interface

Assuming a 3D rectangular domain discretized into block elements with I, J, K elements along the x, y and z axis, respectively, one has a total of IJK elements. Below, the number of collocation point per element interface (P) is computed assuming a homogeneous aquifer.

A.1. Quadratic approximation

Each element has 9 unknowns, thus we have a total of $9IJK$ unknowns. Given the 4 continuity equations at every collocation point, the total number of equations is $4P(3IJK - IJ - IK - JK)$, where P is the number of collocation points per interface. To avoid the creation of an underdetermined inversion matrix, one must have $4P(3IJK - IJ - IK - JK) \geqslant 9IJK$. Therefore, the number of collocation points per interface is: $P \geqslant \frac{9IJK}{4(3IJK-IJ-IK-JK)}$. For $IJK > 4$, $P \geqslant 1$. One collocation point per interface is shown to be sufficient for the quadratic approximation.

A.2. Cubic approximation

Each element has 16 unknowns, thus we have a total of $16IJK$ unknowns. Given the 9 continuity equations at every collocation point, the total number of equations is $9P(3IJK - IJ - IK - JK)$. To avoid an underdetermined system, one must have $9P(3IJK - IJ - IK - JK) \geqslant 16IJK$. Therefore, the number of collocation points per interface P is: $P \geqslant \frac{16IJK}{9(3IJK-IJ-IK-JK)}$. For $IJK > 4$, $P \geqslant 1$. One collocation point per interface is sufficient for the cubic approximation.

Appendix B. Weighting of the continuity equations at the collocation points

Taking $P = 1$, the weights assigned to the continuity equations are computed as the inverse of the ratio of the number of equations to the number of unknowns. A weight of 1 would be if the system is square, such as in solving a boundary value problem to which the method of this study is also applicable, e.g., see Irsa and Galybin (2010). Below, we assume again a homogenous aquifer, a regular block grid, and a limiting case.

B.1. Quadratic approximation

Given the $4(3IJK - IJ - IK - JK)$ equations and $9IJK$ unknowns, the ratio is:

$$\lim_{IJK\to\infty} \frac{4(3IJK - IJ - IK - JK)}{9IJK} = 1.33, \quad \delta(p_j - \varepsilon) = \frac{1}{1.33} \cong 0.75$$

B.2. Cubic approximation

Given the $9(3IJK - IJ - IK - JK)$ equations and $16IJK$ unknowns, the ratio is:

$$\lim_{IJK\to\infty} \frac{9(3IJK - IJ - IK - JK)}{16IJK} = 1.67, \quad \delta(p_j - \varepsilon) = \frac{1}{1.67} \cong 0.6$$

References

Bohling, G.C., Liu, G., Knobbe, S., Reboulet, E., Hyndman, D.W., Dietrich, P., Butler, J.J., 2012. Geostatistical analysis of centimeter-scale hydraulic conductivity variations at the MADE site. Water Resour. Res. 48, W02525. http://dx.doi.org/10.1029/2011WR010791.

Brauchler, R., Doetsch, J., Dietrich, P., Sauter, M., 2012. Derivation of site-specific relationships between hydraulic parameters and p-wave velocities based on hydraulic and seismic tomography. Water Resour. Res. 48, W03531. http://dx.doi.org/10.1029/2011WR010868.

Butler Jr., J.J., 2005. Hydrogeological methods for estimation of spatial variations in hydraulic conductivity. In: Rubin, Y., Hubbard, S.S. (Eds.), Hydrogeophysics. Springer, pp. 23–58.

Camporese, M., Cassiani, G., Deiana, R., Salandin, P., 2011. Assessment of local hydraulic properties from electrical resistivity tomography monitoring of a three-dimensional synthetic tracer test experiment. Water Resour. Res.. http://dx.doi.org/10.1029/2011WR010528.

Doherty, J., 2005. PEST Documentation. <http://www.pesthomepage.org/Home.php>.

Doherty, J., Welter, D., 2010. A short exploration of structural noise. Water Resour. Res. 46, W05525. http://dx.doi.org/10.1029/2009WR008377.

Feyen, L., Ribeiro Jr., P.J., Gomez-Hernandez, J.J., Beven, K.J., De Smedt, F., 2003. Bayesian methodology for stochastic capture zone delineation incorporating transmissivity measurements and hydraulic head observations. J. Hydrol. 271, 156–170.

Fitts, C.R., 2013. Groundwater Science, second ed. Elsevier.

Galybin, A.N., Irsa, J., 2010. On reconstruction of three-dimensional harmonic functions from discrete data. Proc. Roy. Soc. A 466, 1935–1955.

Gellasch, C.A., Bradbury, K.R., Hart, D.J., Bahr, J.M., 2013. Characterization of fracture connectivity in a siliciclastic bedrock aquifer near a public supply well (Wisconsin, USA). Hydrogeol. J. 21, 383–399.

Hyndman, D.W., Harris, J.M., Gorelick, S.M., 1994. Coupled seismic and tracer test inversion for aquifer property characterization. Water Resour. Res. 30 (7), 1965–1977.

Hyndman, D.W., Harris, J.M., Gorelick, S.M., 2000. Inferring the relation between seismic slowness and hydraulic conductivity in heterogeneous aquifers. Water Resour. Res. 36, 2121–2132.

Harbaugh, A.W., Banta, E.R., Hill, M.C., McDonald, M.G., 2000. MODFLOW-2000, the U.S. Geological Survey Modular Ground-Water Model – User Guide to Modularization Concepts and the Ground-Water Flow Process: U.S. Geological Survey Open-File, Report 00-92, 121 p.

Hill, M.C., Tiedeman, C.R., 2007. Effective Groundwater Model Calibration: With Analysis of Data, Sensitivities, Predictions, and Uncertainty. Wiley-Interscience.

Irsa, J., Galybin, A.N., 2010. Stress trajectories element method for stress determination from discrete data on principal directions. Eng. Anal. Bound. Elem. 34, 423–432.

Irsa, J., Zhang, Y., 2012. A direct method of parameter estimation for steady state flow in heterogeneous aquifers with unknown boundary conditions. Water Resour. Res. 48, W09526. http://dx.doi.org/10.1029/2011WR011756.

Kalbus, E., Reinstorf, F., Schirmer, M., 2006. Measuring methods for groundwater–surface water interactions: a review. Hydrol. Earth Syst. Sci. 10, 873–887.

Kobr, M., Mares, S., Paillet, F., 2005. Geophysical well logging, borehole geophysics for hydrogeological studies: principles and applications. In: Rubin, Y., Hubbard, S.S. (Eds.), Hydrogeophysics. Springer, pp. 291–331.

Kowalsky, M.B., Chen, J., Hubbard, S.S., 2006. Joint inversion of geophysical and hydrological data for improved subsurface characterization. Lead. Edge, 730–734.

Labaky, W., Devlin, J.F., Gillham, R.W., 2009. Field comparison of the point velocity probe with other groundwater velocity measurement method. Water Resour. Res. 45, W00D30. http://dx.doi.org/10.1029/2008WR007066.

Lee, En-Jui, He, Huang, Dennis, John M., Chen, Po, Wang, Liqiang, 2013. An optimized parallel LSQR algorithm for seismic tomography. Comput. Geosci. 61, 184–197.

Liu, X., Kitanidis, P.K., 2011. Large-scale inverse modeling with an application in hydraulic tomography. Water Resour. Res. 47, W02502. http://dx.doi.org/10.1029/2010WR009144.

Molz, F.J., Boman, G.K., Young, S.C., Waldrop, W.R., 1994. Borehole flowmeters: field application and data analysis. J. Hydrol. 163 (3–4), 347–371.

Moore, C., Doherty, J., 2006. The cost of uniqueness in groundwater model calibration. Adv. Water Resour. 29, 605–623.

Neuman, S.P., Yakowitz, S., 1979. A statistical approach to the inverse problem of aquifer hydrology: 1. Theory. http://dx.doi.org/10.1029/WR015i004p00845.

Paige, C.C., Saunders, M.A., 1982. LSQR: an algorithm for sparse linear equations and sparse least squares. ACM Trans. Math. Softw. 8 (1), 43–71.

Post, V.E.A., von Asmuth, J.R., 2013. Review: hydraulic head measurements – new technologies, classic pitfalls. Hydrogeol. J. 21, 737–750.

Saltelli, A., Ratto, M., Andres, T., Campolongo, F., Cariboni, J., Gatelli, D., Saisana, M., Tarantola, S., 2008. Global Sensitivity Analysis: The Primer. John Wiley & Sons, Ltd., pp. 292.

Schulmeister, M.K., Butler, J.J., Healey, J.M., Zheng, L., Wysocki, D.A., McCall, G.W., 2003. Direct-push electrical conductivity logging for high-resolution hydrostratigraphic characterization. Ground Water Monit. Remediat. 23 (3), 52–62.

Shapiro, S.A., Audigane, P., Royer, J.J., 1999. Large-scale in situ permeability tensor of rocks from induced microseismicity. Geophys. J. Int. 137, 207–213.

Sun, N.-Z., 1994. Inverse Problems in Groundwater Modeling, Theory and Application of Transport in Porous Media. Kluwer Academic Publishers.

Tang, X.M., Cheng, C.H., 1996. Fast inversion of formation permeability from borehole Stoneley wave logs. Geophysics 61, 639–645.

Wang, D., Zhang, Y., Irsa, J., 2013. Dynamic data integration and stochastic inversion of a two-dimensional confined aquifer. In: Proceeding of the 2013 AGU Hydrology Days. <http://hydrologydays.colostate.edu/Papers_13/Dongdong_paper.pdf> (assessed 07.08.13).

Weir, G.J., 1989. The direct inverse problem in aquifers. Water Resour. Res. 25 (4), 749–753.

Williams, D.M., Zemanek, J., Angona, F.A., Denis, C.L., Caldwell, R.L., 1984. The long space acoustic logging tool. In: Trans. SPWLA 25th Ann. Log. Symp.

Zhang, Y., 2013. Nonlinear inversion of an unconfined aquifer: simultaneous estimation of heterogeneous hydraulic conductivities, recharge rates, and boundary condition. Transport in Porous Media (submitted for publication).

Zimmerman, D.A., de Marsily, G., Gotway, C.A., Marietta, M.G., Axness, C.L., Beauheim, R.L., Bras, R.L., Carrera, J., Dagan, G., Davies, P.B., Gallegos, D.P., Galli, A., Gomez-Hernandez, J., Grindrod, P., Gutjahr, A.L., Kitanidis, P.K., Lavenue, A.M., McLaughlin, D., Neuman, S.P., Ravenne, B.S., Rubin, Y., 1998. A comparison of seven geostatistically based inverse approaches to estimate transmissivities for modeling advective transport by groundwater flow. Water Resour. Res. 34 (6), 1373–1413.